Biogeosciences Discuss., 10, 12417–12449, 2013
www.biogeosciences-discuss.net/10/12417/2013/
doi:10.5194/bgd-10-12417-2013

Biogeosciences
Discussions
Open Access

Flux and accumulation of sedimentary particles off the continental slope of Pakistan: a comparison of water column and seafloor estimates from the oxygen minimum zone, NE Arabian Sea

H. Schulz[1,*] **and U. von Rad**[2,*]

[1]Fachbereich für Geowissenschaften, Paleobiology, University of Tübingen, Hölderlinstr. 12, 72074 Tübingen, Germany
[2]Rosenstraße 19c, 30916 Isernhagen, Germany
[*]formerly at: Bundesanstalt für Geowissenschaften und Rohstoffe (BGR), PF 510153, 30631 Hannover, Germany

Received: 13 May 2013 – Accepted: 22 May 2013 – Published: 23 July 2013

Correspondence to: H. Schulz (hartmut.schulz@uni-tuebingen.de)

Published by Copernicus Publications on behalf of the European Geosciences Union.

Abstract

Due to the lack of bioturbation, the laminated muds from the oxygen-minimum zone (OMZ) off Pakistan provide a unique opportunity to precisely determine the vertical and lateral sediment fluxes in the near shore part of the northeastern Arabian Sea, and to explore the effects of the margin topography and the low oxygen conditions on the accumulation of organic matter and other particles. West of Karachi, in the Hab river area of EPT and WPT (Eastern and Western PAKOMIN Traps), 16 short sediment profiles from water depths between 250 m and 1970 m on a depth transect crossing the OMZ (∼ 120 to ∼ 1200 m water depth) were investigated, and correlated on the basis of a thick, light-gray- to reddish-colored turbidite layer. Varve counting yielded a date for this layer of AD 1905 to 1888. We adopted the young age which agrees with ^{210}Pb- dating, and used this isochronous stratigraphic marker bed to calculate sediment accumulation rates, that we could directly compare with the flux rates from the sediment traps installed within the water column above.

All traps in the area show exceptionally high, pulsed winter fluxes of up to 5000 mg m^{-2} d^{-1} in this margin environment. The lithic flux at the sea floor is as high as 4000 mg m^{-2} d^{-1} , and agrees remarkably well with the bulk winter flux of material. This holds as well for the individual bulk components (organic carbon, calcium carbonate, opal, lithic fraction). However, the high winter flux events (HFE) by their extreme mass of remobilized matter terminated the recording in the shallow traps by clogging the funnels. Based on our comparisons, we argue that HFE for the past 5000 yr most likely occurred as regular events within the upper OMZ off Pakistan. Coarse fraction and foraminiferal accumulation rates from sediment surface samples along the Hab transect show distribution patterns that seem to be a function of water depth and distance from the shelf. Some of these sediment fractions show sudden shifts at the lower boundary of the OMZ. However, the potential effect of the OMZ on carbon preservation in the area would by masked by high mass of fine-grained matter laterally advected, and by the pulsed nature of the resuspension events.

1 Introduction

In the past two decades, after basic knowledge on the sedimentation along the western and eastern margins in the north Indian Ocean had been set by the pioneering study of von Stackelberg et al. in 1972, numerous campaigns and initiatives revealed the key role of the Indian-Pakistan margin sediments in studying the linkages between the production, pathways and preservation of marine organic matter in the ocean environment (Paropkari et al., 1992; Pedersen et al., 1992; Calvert et al., 1995; Schubert et al., 1998; Cowie et al., 1999; Keil and Cowie, 1999, van der Weijden et al., 1999; Schulte et al., 2000; Suthhof et al., 2000). Today, the northern Arabian Sea off Pakistan is characterized by a stable, distinct oxygen minimum zone (OMZ) between water depths of 200 to about 1200 m that impinges on the continental slope. One reason for the very low oxygen concentrations at intermediate depths ($< 0.2\,\mathrm{ml\,L^{-1}}$) is seen in subsequent oxygen consumption by microbial decomposition of organic matter in the water column triggered by the high surface water primary productivity that may depend on the strength and direction of the seasonally reversing summer (southwest) and winter (northeast) monsoonal circulation. There is ample evidence that in the open Arabian Sea the high surface water productivity offshore, and related biogenic fluxes, as well as mineral eolian input is extremely variable, depending on the strength and direction of monsoonal winds (Sirocko and Sarnthein, 1989; Ramaswamy et al., 1991). This particularly holds for the western Arabian Sea under the summer monsoonal low-level jet that causes coastal and ocean upwelling and related high fluxes of settling matter, Vertical fluxes in the open oceanic environment intensely have been studied by means of series of moored and drifting sediment traps (Haake et al, 1993; Nair et al., 1989; Rixen et al., 1999; Pollehne et al., 1993). In contrast, our knowledge on the scales and seasonal timings of the biogenic and abiogenic fluxes down the steep, active margin of the northern Arabian Sea basin, as well as of the roles of the high lateral marine and terrigenous inputs is still fragmentary.

The sediments along the continental slope off Pakistan (Fig. 1a) are characterized by a distinct lamination due to suppressed bioturbation (von Stackelberg, 1972). However, the dysaerobic bottom conditions preventing the sediment from being mixed by burrowing organisms may only be one important factor, in addition to the exceptionally high sedimentation rates of more than 1 mm per year, linked to the high lateral fluxes of remobilized terrigenous and marine matter, as it is observed off the active Makran margin (von Rad et al. 1995; Schulz et al., 1996) off west Pakistan. From sedimentary models on the varve formation and from simple mass calculations we may expect a significant contribution of remobilized matter, laterally advected from the steep continental slopes and from the narrow shelf areas nearby, to add to the particle flux derived from the local biological productivity and thus complicate an identification of the sediment processes. This is corroborated by observation that the sediments from the relatively gentle Indus margin, situated to the southeast of – the steep Makran seem to show more regular patterns in laminae thicknesses. Although laminae in the Indus area generally tend to be thinner and are more difficult to assess, presumably because of the generally lower sedimentation rates in that area, this depositional environment may be better situated to estimate on the roles of vertical and horizontal organic matter flux and its burial and preservation in the sea bed (Schulte et al., 2000).

The steep Hab area to the west of Karachi hosts the most distinct sediment laminae on mm- to sub mm- scales (von Rad et al., 1995) at OMZ- water depths. At least for the past 5000 years there is a continuous deposition of annual “varved” couplets, which point to a strong seasonality in the amount and composition of material settling to the sea-floor (von Rad et al., 1999). Microscopic analyses of thin-sections show distinct alternations of dark-colored organic-carbon rich and light-colored organic carbon-poor laminae which suggest a cyclic pattern due to changes in the flux and composition during summer and winter at the Makran (Schulz et al., 1996, von Rad et al., 1999; Berger and von Rad, 2002; Lückge et al., 2002). Numerous studies have shown that the organic matter is almost entirely of marine origin in the Pakistan slope area, with little contribution of terrestrial organic carbon (OC) from the poorly vegetated hinterland (Cowie et al., 1999; van der Weijden et al., 1999).

High sedimentation rates by lateral advection my play in important role in rapidly sealing organic matter on the sea floor from exposure to bacterial activity and in-situ degradation that may favor the accumulation of organic matter (Suthhof et al., 2000). These authors showed that the duration of oxic degradation to be lowest within the mid-depth of the OMZ, as a function of local productivity, mass accumulation rate (AR) on the sea floor and degradation in the water column (exposure time). These interfering effects may result in a zone of relatively "young", less degraded OC matter to be centered at 800 m water depth in area B, some 100–200 m shallower than in the Indus area. In contrast, a study including 3 stations from the Hab area showed a positive effect of low bottom water oxygen on the sorption of organic carbon particles (OC) onto mineral surfaces, defined by their surface areas (SA) (Keil and Cowie, 1999). However, the mineral surface areas are negatively correlated to grain size, which suggest that grain size variations of the sediments might be important (Keil and Cowie, 1999). Their findings are corroborated by the study of van der Weijden et al. (1999) on OMZ-sediments isolated from the margin further offshore, where OC/SA ratios were found more than twice (up to 5.7) than at the margin (< 2.3). This would suggest a dilution effect along the margin, possibly by the admixture of a certain fraction of poorly sorptive mineral matter, or an overall masking overprint of preservational effects by the high amount the laterally advected, allochochtonous matter.

Quantitative estimates are needed to better describe the complex sedimentation processes at the continental margin off Pakistan. In the present study, we will focus on the determination of accumulated sediments along a depth transect in the Hab area between 200 and 2000 m water depth, and will compare these rates of accumulation with the flux estimates derived from sediment traps from the overlying water column. Published estimates of surface water productivity potentially can be used to better describe quantitatively the locally produced flux of OC from primary production (Sarnthein et al., 1992). However, this approach may not be valid in the near-coastal environment where lateral fluxes are high and may temporally dominate. To better determine their role, we will focus on possible differences in the amount and preservation of bulk fractions of biogenic and mineral matter found above, in the center and from below the OMZ. The concentration and accumulation of the main sand-sized components preserved along our depth transect crosscutting the OMZ may be used to provide additional information.

2 Geologic setting and previous investigations

20 box grabs and 6 multicores, taken in 1993 during cruise SONNE 90 (von Rad et al., 1995) and in 1995 during METEOR cruise M32/2 (Schott et al., 1996), recovered undisturbed top sediments from water depths between 96 m and 2881 m from the narrow area at the contact zone of the active Pakistan margin with the Indus margin close-by to the SE, where the broad shelf characterizes the passive Indian margin (Fig. 1b). This forms an extremely complex triangular basin, opening to the W-SW within the NE-corner of the Arabian Sea and was named “Area B” = “Hab Transect” by von Rad et al., 1995 in their initial study (see Fig. 1c). The depositional environment of that region can be characterized in terms of four distinct tectono-sedimentologic settings: (1) bordered to the North by the steep Makran margin as part of the accretionary complex, where the incoming oceanic crust is covered by thick wedges of accreted sediment prisms that tend to be eroded and redistributed to the lower parts of the wedge (stations 39, 53). (2) a lower accretionary zone with rather regular topography of structural valleys and highs on vertical scales of some 100 m due to the imbrication of thrust slices of some km to tens of km in size (stations 1, 35, 58–158). (3) a more gentle NE-slope of slumped sediments from the Murray Ridge on top of the basaltic abyssal plain floor of the Arabian Plate to the south (stations 2-6, 42–46, 54). This latter is drained by a few relatively large, deep ENE-WSW trending channels that eventually form hanging valleys, with their upper ends draining the Indus shelf that might structurally belong to a melange zone between the southern Murray Ridge and the Indus Shelf that is based

on continental crust. The short sediment profiles are thus geographically distributed on three different structural units.

In the near surface sections of 16 box- and multicores, an up to 12-cm thick whitish- or reddish-colored silt-clay layer was identified, that could be traced over a large area of the Hab transect, possibly covering an area of some 1000 and 600 km^2, respectively. In addition to the strong visual contrast between the two homogeneous OC-poor, centimeter-thick silty layers to the over- and underlying laminated sediment (Staubwasser and Sirocko, 2001), the two types of fine-grained clastic layers seem to display a regional distribution with the white layers to be found more in the north of the NE-SW trending channels. To this end, all laminated Sonne cores (except station 35 at 416 m) showed a distinct, OC-poor red-colored turbidite layer, always above the white layer (see their "red layer" in Fig. 3a of Staubwasser and Sirocko, 2001). This reddish-colored type of sediment, sometimes showing fining upward structure or indistinct internal laminations, was previously described by Schulz et al. (1996) and von Rad et al. (1999) to occur sporadically also in the longer piston and kasten cores of the area, and was interpreted to represent episodic event deposits (their type "F-turbidite") of fluvial matter possibly linked to periods of strong rainfalls or floods in the hinterland. Staubwasser and Sirocko (2001) in more detail investigated the light-grey clastic layers and concluded that these might consist of expulsed by mud-volcanoes of the active Makran margin. This view, however, was strongly refuted by von Rad et al., 2002. These authors argued that the distinct-light grey layers are better explained as "plume deposits" representing riverine suspensions from episodic floods on the Makran. However, the significance of the white/light gray layer from versus the red dish turbidite (in addition to their different color and texture) is only weakly supported by geochemical data. Staubwasser and Sirocko (2001) for example report only insignificant differences in concentrations of 0.56 vs. 0.64 (% OC) or 11.7 vs. 10.8 (% $CaCO_3$) and of most trace elements. Unfortunately, grain sizes for the two types of layers were not presented. Following these authors, the red color results from finely dispersed hematite based on their XRD data. According to von Rad et al., 1999, the light-grey colored clay-silt layers represent sus-

Title Page
Abstract | Introduction
Conclusions | References
Tables | Figures
◀| |▶
◀ ▶
Back | Close
Full Screen / Esc
Printer-friendly Version
Interactive Discussion

pensate deposits, named by these authors as C-layers. The near surface deposition of distinct layers of clay-silt can be followed within almost all short sediment cores taken during three cruises in the Hab area, as the same stratum was sampled in 1998 again by box- and multicores 268 MC, 605 m water depth; 276 KG, 780 m; 262 MC, 875 m; 291 MC, 902 m of Sonne cruise 130 (von Rad et al., 1998).

Here we further present numerical flux data for TOC, biogenic opal and $CaCO_3$ analyses from the Western and Eastern PAKOMIN Trap stations (Fig. 1c) that were deployed within and below the OMZ and sampling depths of 534 m and 1466 m (WPT-shallow and WPTdeep) and at 590m (EPT1 and EPT2, see Table 2). Unfortunately, none of the four deployments sampled the entire programmed period we wished to obtain, covering all seasons of the Indian monsoon. All traps stopped collecting particles in winter with the last cups between the first half of January and the end of February almost filled. Fluxes were extremely high towards the end of each trap run, with a generally increasing relative fraction of lithogenic flux towards the ends (Andruleit et al., 2000; Schulz et al., 2002). The remaining cups of the series were empty. It is important to notice, that all four traps had rotated cups below the funnel completely. It is suggested that due to a large flux of matter cups and possibly even the funnel had been filled up to with sediment resuspended from the margin during these "last" one or two sampling periods before the traps the clogged finally (Andruleit et al., 2000; Schulz et al., 2002). It is suggested that the traps after the vigorous winter sedimentation event did not stay in upright position in the water column. However, because of the lack of direct observations, finally we can only speculate on the possibly reasons preventing the traps from collecting material further (see discussion).

3 Material and methods

3.1 Sediments and age control

The organic carbon (OC), opal and carbonate ($CaCO_3$) concentrations were determined following Dietrich and Marchig (1995) and Suthhof et al. (2000). The composition of the coarse fraction larger than 150 microns (µm) in core top samples was counted from a few ml of freeze-dried sediment from the top centimetre washed through a 63 µm mesh. The residue was dried at 60 °C and sieved into six sub-fractions of 63–150, 150–200, 200–250, 250–315, 315–400 and > 400 µm, respectively. The five splits of at least 70 grains from these fractions (> 150 µm) were obtained with a Otto-micro splitter for each sample. In these splits all grains were identified following the categories: (1) inorganic compounds (quartz, mica, oxides, lithic grains; Inorg.), (2) megafossils (sponge spicules, ophiurid remains, pteropods, fish debris etc.; Megaf.), (3) siliceous tests (large radiolaria, diatoms, silicoflagellates; Silic.), (4) planktonic foraminiferal debris, (P.F. debris); (5) intact planktonic foraminiferal tests (P.F.); and (6) benthic foraminifera (B.F.). The relative abundances (in %) and the absolute abundances (specimens per gram of dry sediments, spec./g) of the foraminiferal species and of the other components were calculated separately for the different size fractions. Here, we present the abundance data based on the fraction > 150 µm.

The short sediment cores, taken off the box corers on board of Sonne cruise 90, were sealed and were stored cool at BGR Hannover. Before opening the cores, the profiles of sediment magnetic susceptibility and γ-ray attenuation were analyzed at 0.5 cm-intervals using a GEOTEC-multisensor core logger (Schultheiß and Weaver, 1992). Alternatively, discrete samples were taken at 1–2.5 cm-intervals by 10 ccm-syringes from sliced sediment profiles in order to determine the sediment physical properties of sand fraction, natural water content, wet bulk and dry bulk density. The latter two were calibrated against parallel profiles of γ-ray attenuation, which is known to vary as a function of sediment density (Weber et al., 1997). Using these calibrations from selected cores, a homogenous set of dry bulk density data from 15 sediment profiles of 12 to 53 cm length from water depths of 250–1970 m was generated. The 30 cm-long multicore M32-MC2 from the depth 197 m was described only visually prior to sampling, and showed a homogenous light-colored layer of silty clay between 18.0 and 21.0 cm core depth (Schott et al., 1996).

A detailed varve chronology has been developed for the laminated sediments from the Pakistan Margin (Schulz et al., 1996; von Rad et al., 1999). In short, these chronologies are based on the interpretation of light-colored, grey (winter) and dark-colored (dark gray-olive gray) summer layers. This interpretation was verified by the observation that 5 light-dark couplets accumulated at the upper Makran margin within the period of 1993 (Sonne 90) to 1998 (Sonne 130), representing recurrent suspension events linked to the high winter precipitation and to the high productivity during summer SW-monsoon (Lückge et al., 2002).

About 150 samples from the top 20 cm of laminated sediment at narrow intervals of in selected cores MC1, 3, 5 and KGs 39, 58) were used for lead-210 Pb-dating to precisely determine the sedimentation rates of the last 150 years. These data are presented here only for core 58 KG (Erlenkeuser, unpublished data). Analytical details of the ^{210}Pb method are outlined in Erlenkeuser and Peterstad (1984).

AMS^{14}C ages of monospecific samples of *Globigerinoides ruber* (white) or of mixed P.F. were determined the Leibniz Labor Kiel, Germany.

3.2 Sediment traps

We used four trap moorings of type MARK 7G-2l at WPT (24°36′ N, 65°35′ E; 2004 m water depth) and EPT (24°46′ N, 65°49′ E; 1099 m) (von Rad et al., 1995; Schott et al., 1996). Collecting time was programmed from October, 15th 1993 to February 1994 and from May 1995 to February 1996 (EPT2). Sampling intervals for the 18 cups used in the present study were 22 days for WPT and EPT1, and 24 days for EPT2, respectively. The total mass fluxes, the carbonate and lithogenic particle fluxes of some of these moorings have been presented by Andruleit et al. (2000) and by Schulz et al. (2002) who studied the coccolithophore and planktic foraminiferal fluxes. Details of trap and sample preparation, TOC, $CaCO_3$, biogenic opal analyses of the trapped material, and of the derivation of fluxes are described in Haake et al. (1993) and Andruleit et al. (2000).

3.3 Calculation of fluxes

In order to obtain a quantitative measure on the flux of individual particles and compounds to the seafloor, accumulation rates (AR) were determined for the 16 short profiles, based on the sedimentation rate estimates from cores and dry bulk densities following Thiede et al. (1982):

$$\mathrm{AR}_{\text{bulk sediment}} = \mathrm{SR}\,\rho_{\text{dry}} \tag{1}$$

with AR in $\mathrm{g\,cm^{-2}\,kyr^{-1}}$, SR in $\mathrm{cm^{-2}\,kyr^{-1}}$, and ρ_{dry} in = $\mathrm{g\,ccm^{-3}}$.

The accumulation rate of the individual compounds, of the individual sediment components in the sample is calculated as follows:

$$\mathrm{AR}_{\text{component}} = \mathrm{SR}\,\rho_{\text{dry}}C/100 \tag{2}$$

where the concentration, C, is the fraction, or the number of the specimens, in % of the dry weight.

Estimates of local primary productivity were adopted from Antoine at al. (1996). All flux and accumulation rate estimates are listed in Table 2. Most estimates for the study are expressed as $\mathrm{mg\,m^{-2}\,d^{-1}}$ or spec $\mathrm{m^{-2}\,d^{-1}}$ to allow for direct comparison.

4 Results

4.1 A turbid layer as synchronous stratigraphic marker

The 5 to 12 cm-thick, fine-grained silty layer was observed in a number cores at 10 to 25 cm sediment depth of the Hab transect. On the basis of sediment color, TOC content, and other sediment parameters (percent water content, wt.% coarse fraction, sediment density). This distinct turbid layer (see examples for selected cores from OMZ depths of 247 m, 386 m, 704 m, 876 m; Figs. 2a–d) could be traced over a large area and over the entire depth range of the OMZ. Within the upper OMZ, i.e., between about 250 and 900 m water depth, normal grading was eventually observed in this layer with sharp contacts to the laminated sediments above and below. As seen in the high-resolution density data (Fig. 2a, d) the upper, red layer shows internal details with highest density to the bottom that might reflect coarser grain sizes or compaction at the base. Sand content of this turbidite is extremely low and coincides with low OC. Due to increasing bottom water-O_2 concentrations that allow for macrofaunal bioturbation, that layer at depths above and below the OMZ could only be determined with less precision. There is still a slight relative increase of maximum in density in the high-resolution logs of sediment density below a sediment depth of 5–6 cm found at a water depth of 1970 m (Fig. 3). Although the sedimentation is characterized by the deposition of up to some mm- to cm-thick light-colored turbid layers (Schulz et al., 1996), no other red layer was found in the upper meters of sediment in the Hab area. We assume that this turbid layer reflects a synchronous depositional event that can be ideally applied as a regional marker bed for core correlation.

4.2 Local sedimentation rates by varve chronology, Pb-dating and ^{14}C-Ages

Counting and measurement of the individual thicknesses of the couplets of laminae, including replicate runs, yielded an age of the thick red layer (F-turbidite) of 1888 AD and 1905 AD in 39 KG and 58 KG, respectively. This difference is well within the rage of uncertainties of 10 %, that may be caused in most cases be overlooking extremely thin layer couplets (von Rad et al., 1999). However, ^{210}Pb-dating of core 58 KG and of other short sediment profiles indicate that the younger date of 1905 AD is reliable, based also on varves deposited during the last 100–250 years that were counted in other core profiles. The datum of 1905 AD suggest sedimentation rates of 167 cm ky^{-1} and 150 cm kyr^{-1}, whereas, by the correlation via the marker horizon, sedimentation rates at shallow depth are distinctly higher, (up to 272 cm ky^{-1}) and in general lowered at depth (stations 46 KG and 144 KG, 44 cm ky^{-1}) (Table 2). In order to further support our stratigraphic model, the AMS-radiocarbon ages from intervals from above and below the red layer in cores M32MC1 and M32MC5 show a difference of 40 ^{14}C-years over the interval of 7.3 cm in the latter core. This fits to our suggested sedimentation rate of 183 cm ky^{-1}. Further, the dates of the laminated intervals can be used to assess the local radiocarbon ages of the surface water, since this “reservoir effect” is known to was highly variable in space and time. As expected, the radiocarbon dates of the top sediments of MC1 and MC5 yielded negative ages caused by the post-bomb high levels of atmospheric radiocarbon concentrations (Table 1). In contrast, the three laminated intervals in cores MC1 and MC5 from the OMZ yielded uncorrected, “conventional” ^{14}C ages of 747 ± 27 and 664 ± 25, 705 ± 23 years, respectively, that correspond to varve ages of 1820 AD, and 1903 AD, 1867 AD. From the difference between the varve ages of 175 BP, 92 BP and 128 BP of these depth intervals clearly date to the pre-bomb time, and the corresponding “conventional” ^{14}C ages, we could determine rather uniform reservoir ages of 582 and 572, 577 years from the three different ^{14}C dates. This average reservoir age of 577 years is different from the 640 years used by von Rad et al. (1999).

4.3 Sedimentation patterns

4.3.1 Sand fraction analysis across the OMZ

The sediments on the continental margin off the coast of Pakistan can be described as organic-rich, carbonaceous silty clays with typically 1–2 % of OC and 15–30 % of $CaCO_3$. An exception is the carbonate-rich facies of relict sands on the shelf, which have a significant component biogenic calcite and a bulk carbonate content of up to 70 % (von Stackelberg, 1972). These carbonate sands are restricted shallow water depth of < 200 m depth on the Makran side, but are found down 400 m on the Indus side. The flat shelf morphology may provide space and substrate for sessile carbonate producers, which is seen in high relative abundance of Megaf. (Fig. 4) at > 250 m water depth. Below that depth, the sand fraction decreases to about 0.5–3.0 weight-%, where most of the coarse fraction is made up of planktonic and benthic foraminiferal tests with a few hundred to thousand tests per gram dry sediment. Remarkable for sediments in the OMZ is the high abundance of benthic foraminifers. The faunal associations constitute only a few species and indicate a stressed environment at the depth of the OMZ. Zobel (1973) made a distinction between a shallow-water Uvigerina-Cassidulina facies and a Buliminacea facies in the middle of the OMZ. Endobenthic foraminifera dominate the OMZ-sediments, nearly barren of epibenthic forms. The accumulation of benthic foraminiferal shells is highest in the shallow waters of the shelf areas with a maximum on the outer shelf, and a sharp decrease above the shelf break. The same holds for the accumulation of P.F. shells and also for the P.F. debris. The highest abundance of inorganic components (mainly quartz grains and concretions) was found above the shelf break, but also at mid-OMZ depth in the Hab area. In contrast to other high-productivity areas, siliceous microfossils (diatoms, radiolarians, silicoflagellates, sponge spicules) are very rare in the sand fraction of surface sediments which contain about 4–5 wt.% of opal. In general, the abundance and relative frequencies of siliceous tests in the coarse fraction increase with depth, (Fig. 4a and b; Silic.), however no clear pattern is seen in the accumulation possibly because the low numbers of less than 100 individuals per gram dry sediment. Pyrite, an indicator of anoxic conditions, was found only sporadically, filling the spherical tests of the planktonic foraminifer *Orbulina universa*.

Apparently the lower boundary of the OMZ coincides with major changes in several properties of the sand fraction. For instance there are clear patterns of increases in the AR of Inorg., P.F. debris, and P.F. Other shifts include decreases of the relative fraction of Megaf. and maxima of the same parameter near the lower OMZ boundary which all indicate that the OMZ has a strong impact on the accumulating material and for benthic life. For instance, there is a sharp minimum in the frequency and sedimentary concentration of B.F. (Fig. 4, B.F.). This minimum is opposed to a maximum in relative abundance of P.F., the latter group making up to 80 % of the sand fraction immediately below the OMZ where also an increase in the accumulation of P.F. (Fig. 4c) is noted. A strong reduction of B.F. at the lower boundary of the OMZ was observed by Zobel (1973). She explained this gap by a change to a specific benthic community characterized by low population densities at the interface between the Buliminacea facies and the more oxic deep water Bulimina aculeate facies. However, based on accumulation rate, we can clearly state that the B.F. population at the lower boundary as a whole show stable numbers. Only the P.F. strongly increase in numbers (together with Inorg, P.F. debris and possibly Silic. (Fig. 4c), thus causing a dilution effect on the B.F. For the planktic foraminiferal fragmentation we observe parallel shifts to the frequency of P.F. (Fig. 4a), that that foraminiferal dissolution is not enhanced immediately near the lower boundary of the OMZ. The maximum of AR P.F. debris in the lower marge of the OMZ and immediately below coincides at that depth level of increases in the AR of Inorg. (Fig. 4c).

OMZ sediments in the center seem to be characterized by a higher absolute number of P.F.debris, the accumulation of inorganic parties that can be interpreted as precipitates, but also by enhanced accumulation of Megaf, P.F. and B.F, when compared to hemipelagic sediments offshore. In contrast, the upper boundary of the OMZ is governed by the high vertical fluxes at the outer shelf and transport of allochthonous matter and macrofossil shells down the margin.

4.3.2 High accumulation rates of bulk parameters OC, $CaCO_3$ and opal

Counting of the varves in various core profiles and lead-210 dating both yielded an age of about 90–100 years for the turbiditic red layer. Sedimentation rate has a strong impact on the respective accumulation rate (see Eq. 1), as changes in dry bulk density are relatively small. The thirteen density profiles show a rather uniform density of ~ 1.0 of the turbid layer used for correlation. Density profiles from above that layer show values increasing with water depth. Most density profiles for the past ~ 100 years from OMZ depths show values of $< 0.6\,\mathrm{g\,cm^{-3}}$ with a mayor shift between Site 76 KG and MC1 (Fig. 3) and densities of $> 0.7\,\mathrm{g\,cm^{-3}}$.

A general decrease of SR and hence, of AR is observed with water depth (Suthhof et al., 2000). Individual sites at the upper margin show a large variability with highest AR_{bulk} of > 4000 mg (Fig. 5). In contrast, the two sites 44 and 42 display only half of that flux, as MC 5 again shows a slightly higher AR_{bulk} of 2600 mg m^{-2} d^{-1}. It is important to notice that the mentioned sites within the uppermost OMZ are still situated within a relatively flat morphology, as the shelf edge of that area is as deep as 400 m below present sea level. Thus, all sites above ~ 400 m are located within the OMZ that is bathing a substantial part of the shelf. AR on the shelf are highest and show largest variability with 1800–3500 mg m^{-2} d^{-1}. MC6 from the same area is the uppermost site on the slope and displays relatively low AR_{bulk} of 1300 mg m^{-2} d^{-1}, Table 2). The deeper sites 39 KGff. all are situated on the Makran side of the Hab profile. Again these sites show in general a decrease of AR_{bulk}, with a decline from > 2600 mg m^{-2} $^{-1}$ to ~ 1300 mg m^{-2} d^{-1} with water depth (Fig. 5a). This of trend in general hold for all bulk parameters (Fig. 5b, c) except for the sedimentary concentration of OC (Fig. 5d), that is distinctly lowered at the uppermost sites at the Indus side of the investigated Hab transect. In contrast, $CaCO_3$ has a very high relative and absolute accumulation on the upper shelf, where its relative fraction is about 25 %. At deeper depths, this ration decreases to less than 10 % (Table 2). A negative correlation between OC and the low bottom water oxygen within depths of the OMZ cannot be observed.

4.4 Incomplete time series of fluxes in the water column compared with sea floor accumulation rates

Unique environmental conditions may prevail off the slope of Pakistan. The longest traps time series (EPT-2, see Table 2) collected particle from late spring (May 1995) to late winter stopped immediately in February 1995. An extremely high bulk particle flux of 2000 to > 5000 mg m^{-2} d^{-1} was also measured during the three short sampling in intervals of shallow traps EPT1 and WPTs and at WPTd (Fig. 6a). The latter trap had the shortest period of collection of less than three months, between October and mid-January (Table 2): trap WPTd apparently was affected by this extreme flux as collection was stopped, although no increase in winter flux is noticed for that trap. We here define the onset of the winter high flux period (HFP) by the dramatic increase in bulk flux (Table 2). As we may show in the following, the HFP can be considered as a regular phenomenon of the area, despite the timing of the start of HFE period is slightly different for the individual series: In EPT2 the shift is observed from collection period 10 to 11 (10 January 1996). In EPT1 an increase is noticed in sampling number 3 and the strong shift is from cup 4 to 5 (20 December 1993). For the deployment of the same year further offshore (WPTs and WPTd programmed to sample flux simultaneously to EPT1 inshore), the start of HFP is only recorded at the shallow trap WPTs and is one collection period (22 days) later (sampling number 4). The average flux of the short period are distinctly higher in the EPT trap, the one closest to the coast, than in the two WPT traps further offshore (Fig. 6b). In the trap WPTd deployed at 1466 m the flux is lower for that period than in the shallow trap WPTs at 534 m.

The particle flux in the Hab area of Pakistan is about 10 times higher than in the open ocean areas of the Arabian Sea (Haake et al., 1993). Moreover, the fluxes within the water column, which could be determined only for a limited period of time, agree surprisingly well with the accumulation rates measured at the seafloor. In both environments, the bulk flux amounts to several 1000 $\mathrm{mg\,m^{-2}\,d^{-1}}$, and the $CaCO_3$ and TOC fluxes range from to several tens of $\mathrm{mg\,m^{-2}\,d^{-1}}$ to several 100. High winter flux observed at shallow water depth is as high or even higher (3500–5000 $\mathrm{mg\,m^{-2}\,d^{-1}}$) and in the same order of magnitude as AR estimated on the shelf (Fig. 5). The highest trap flux during summer SW-Monson is recorded in EPT2-06. It is characterized be a high fraction of OC (%), whereas all winter fluxes show relatively low OC fractions. This contrasts with the high lithic fraction and high overall flux of the HFE. An analysis of the coarse fraction of EPT2 support the origin of remobilized matter from the shallow depth: small benthic foraminifera make up to 10 % of the foraminiferal flux during the winter high flux event, presumably taken up from the shelf (Schulz et al., 2002).

5 Discussion and Conclusions

Among the various data sets generated on the bulk sediment and on the different types of components, the reconstruction of quantitative data (Table 2, Fig. 7) allow for direct comparison between sea floor and water column estimates to discuss and interpret the processes behind. Calculation of fluxes requires accurate dating and precise determination of sediment accumulation sates. It would be expected that sedimentation rates are highly variable in an active continental margin setting. We approached these problems by the identification and dating of an isochronous marker bed at ~5–25 cm sediment depth in the laminated dysoxic to suboxic sediments of Pakistan, where sediment profiles are largely intact, with only minor smoothing by bioturbation (Fig. 3). A general trend of decreasing accumulation with water depth is evident. High flux on the shelf and down the upper margin is not exceptional, but rarely monitored in scales of years to decades by series of sediment profiles in the highly dynamic continental coastal and margin zones with high vertical and lateral shifts of depocenters (Fig. 5). Due to the rapid uplift and rugged topography, sedimentation is characterized by resedimentation processes and downslope deposition of fine-grained sediment predominantly at the Makran side. This may explain the relatively high flux at stations 39 KG, 53 KG and 58 KG (2400–2600 mg m^{-2} d^{-1}) when compared to the next shallower stations taken from the Indus side (Figs. 1, 5). The disturbing effects may reason the poor numbers of sediment trap moorings installed at coastal and continental margin sites to record the highly dynamic flux (Fig. 6). A rather good overview of sediment traps may be taken from the planktonic foraminiferal study of Zaric et al. (2006) who reported only one from an shallow environment of an open margin from water depths < 1000 m out of 41 casts. For the available four time series EPT1, EPT2 and WPT1s, WPT1d off Pakistan, we stress the observation that none of these deployments completed the programmed collection periods although rotating, because all traps at the shallow water depths of 534–590 m were clogged and stopped collecting matter during dramatic shifts in flux by a factor of 10 to 20. The exact timing of increases in flux is different for the three traps, but seem to follow a sequence of events all triggered by the HFP. The best explanation for the relatively early break at the deep trap record WPTd (Fig. 6a) is the high load of the settling sediment (effecting the clogging of EPT1 and WPTs) that may have dragged or even may have turned upside down the lower trap at the moment of open cup 4 that was losing some of the material collected immediately before. If so, the dense lithogenic matter would have preferentially left the open cup with the light organic staying inside, before the trap rotated to cup 5ff. that remained empty or recorded only insignificant flux (Fig. 6b). In contrast, the two shallow traps EPT1 and WPTs were clogged. Only extremely small amounts of the HFE was successively sinking down into the cups rotating, showing a "similar but not fully parallel development" as described from the post HFE-time series of WPTs by the study of coccolithophore fluxes (Andruleit et al., 2000).

We observe that the fluxes of WPTs and WPTd show a coherent pattern of sampling for the first three intervals; after 20.12. the flux within the shallow trap EPT near to the upper margin at 590 m trap depth dramatically increased, which is observed, one sampling interval later in WPTs but is not seen at WPTd at 1466 m.

The sharp pulse of fluxes at the shallow water indicates that the upper open water column had been loaded with sediment suspension, more than 30 km distant from the shelf edge. In the two sediment traps (EPT and WPTs) only the first six "cups" were filled. Therefore, these samples represent only the period of an intermonsoon phase and of the northeast monsoon from the middle of October 1993 to the middle of February 1994. We may speculate that the longest time series EPT 2 must have received have HFE received a high pulsed flux of 23000 to 30000 mg m^{-2} d^{-1} to balance the averaged fluxes of only 750 mg m^{-2} d^{-1} during the rest of the year to fit to the ~ 2000 to 2500 mg m^{-2} d^{-1} of flux that we reconstructed from sediment stations MC1 and 58 KG near the EPT1 and EPT2 moorings. Moreover we may speculate on the maximum flux that affected the margin in the past ~ 200 yr using the thick age marker bed. For that 5 to 10 cm-thick event bed, by a density of 1 g cm^{-3} (Fig. 3), we may calculate a AR of 15000 to 30 000 mg m^{-2} d^{-1} that is 5 to 10 times of the winter flux required to equal to average flux record for the past 90–100 years in the sea bed. No similar layer has been found in the varved record of the Hab area during the past 5000 years (Schulz et al., 1996; von Rad et al., 1999; Berger and von Rad, 2002). This may argue for the relatively stable fluxes during the HFE in the late Holocene,.

In the near-shore area within the OMZ, the bulk accumulation rates are almost twice as high as below 1000 m w.d. and support that the major source of materials from shallow water depth (Fig. 7). The accumulation rates of the biogenic components $CaCO_3$, opal (not figured) and TOC follow this trend (Table 2). Atlas values show highest PP off 750 mg OC m^{-2} d^{-1} at the shelf edge (Antoine et al., 1996) off the steep Makran coast which is consistent with faunal observations (Suthhof et al., 2000). The accumulation rates of OC, however, decrease with water depth by a factor of 3–6. Below the OMZ, they are relatively constant (about 10 OC mg^{-2} d^{-1}); between 900 and 250 m water depth, however, the rates vary between 30 and 90 mg OC m^{-2} d^{-1}. There is no distinct OC maximum in the sediments on the sea floor (neither in the percentages nor in the accumulation rates). The decreasing AR OC with water depths contrast to the uniformly low oxygen values of the OMZ. The elevated productivity near-shore, associated with an elevated lateral input of resuspended organic material, and its rapid burial on the seafloor during the HFE seem to be the controlling factors for OC deposition in the area off the coast of Pakistan.

Acknowledgements. We thank Birgit Stenschke, Martina Schmidtke for laboratory assistance, Helmut Kawohl and Rainer Goergens for obtaining high-quality sediment cores, Captain Papenhagen and Captain Kull and their skilled crews for help and good collaboration on board of R.V. SONNE and R.V. METEOR. The first author wishes to express his sincere thanks to the Hamburg group of marine biogeochemistry around Venu Ittekkot, Andreas Suthhof, Jörg Tiemann, Martin Wiesner, and Birgit Gaye for discussions and support. This study was funded by the German Federal Ministry of Education and Research (BMBF), Projects 03G0090A, 03F0137C and 03G0806C (CARIMA).

References

Andruleit, H. A., von Rad, U., Bruns, A., and Ittekkot, V.: Coccolithophore fluxes from sediment traps in the northeastern Arabian Sea off Pakistan, Mar. Micropaleontol., 38, 285–308, 2000.

Antoine, D., André, J.-M., and Morel, A.: Oceanic primary production, 2. Estimation at global scale from satellite (coastal zone color scanner) chlorophyll, Global Biogeochem. Cy., 10, 57–69, 1996.

Berger, W. H. and von Rad, U.: Decadal to millennial cyclicity in varves and turbidites from the Arabian Sea: hypothesis of tidal origin, Glob. Planet. Change, 34, 313–325, 2002.

Calvert, S. E., Pedersen, T. F., Naidu, P. D., and von Stackelberg, U.: On the organic carbon maximum on the continental slope of the eastern Arabian Sea, J. Mar. Res., 53, 269–296, 1995.

Cowie, G. L., Calvert, S. E., Pedersen, T. F., Schulz, H., and von Rad, U.: Organic content and preservational controls in surficial shelf and slope sediments from the Arabian Sea (Pakistan Margin), Mar. Geol., 161, 23–38, 1999.

Dietrich, P. G. and Marchig, V.: Sedimentation and early diagenesis in the area of the oxygen minimum off the Indus River (Pakistan, Arabian Sea), Zentralblatt für Geologie und Paläontologie Teil I, 1/2, 45–61, 1995.

Erlenkeuser, H. and Peterstad, K.: Recent sediment accumulation in Skagerrak as depicted by 210-Pb-dating, Norsk Geologisk Tidsskrift, 64, 135–152, 1984.

Haake, B., Ittekkot, V., Ramaswamy, V., Nair, R. R., and Curry, W. B.: Seasonality and interannual variability of particle fluxes to the deep Arabian Sea, Deep-Sea Res., 40, 1323–1344, 1993.

Keil, R. G. and Cowie, G. L.: Organic matter preservation through the oxygen minimum zone of the NE Arabian Sea as discerned by organic-mineral interactions, Chem. Geol., 161, 13–22, 1999.

Lückge, A., Reinhardt, L., Andruleit, H., Doose-Rolinski, H., von Rad, U., Schulz, H., and Treppke, U.: Formation of varve-like laminae off Pakistan: decoding 5 years of sedimentation, in: The Tectonic and Climatic Evolution of the Arabian Sea Region, edited by: Clift, P. D., Kroon, D., Gaedicke, C., and Craig, J., Geol. Soc. Spec. Publ., 195, 421–431, 2002.

Paropkari, A. L., Babu, C. P., and Mascarenhas, A.: New evidence for enhanced preservation of organic carbon in contact with oxygen minimum zone on the western continental slope of India, Mar. Geol., 111, 7–13, 1993.

Pedersen, T. F. and Calvert, S. E.: Anoxia versus productivity: what controls the formation of organic-carbon-rich sediments and sedimentary rocks?, Amer. Assoc. Petr. Geol. Bull., 74, 454–466, 1990.

Pedersen, T. F., Shimmield, G. B., and Price, N. B.: Lack of enhanced preservation of organic matter in sediments under the oxygen minimum on the Oman Margin, Geochim. Cosmochim. Ac., 56, 545–551, 1992.

Nair, R. R, Ittekkot, V., Manganini, S. J., Ramaswamy, V., Haake, B., Degens, E. T., Desai, B. N., and Honjo, S.: Increased particle flux to the deep ocean related to monsoons, Nature, 338, 749–751, 1989.

Pollehne, F., Zeitschel, B., and Peinert, R.: Short-term sedimentation patterns in the northern Indian Ocean, Deep-Sea Res. Pt.II, 40, 737–752, 1993.

Ramaswamy, V., Nair, R. R., Manganini, S., Haake, B., and Ittekkot, V.: Lithogenic fluxes to the deep Arabian Sea measured in sediment traps, Deep-Sea Res., 38, 169–184, 1991.

Rixen, T., Haake, B., and Ittekkot, V.: Sedimentation in the western Arabian Sea, The role of coastal and open-ocean upwelling, Deep-Sea Res. Pt. II, 47, 2629–2651, 1999.

Sarnthein, M., Pflaumann, U., Ross, R., Tiedemann, R., and Winn, K.: Transfer functions to reconstruct ocean paleoproductivity: a comparison, in: Upwelling Systems, Evolution since the Early Miocene, edited by: Summerhayes, C. P., Prell, W. L., and Emeis, K.-C., Geol. Soc. Special Publication, 64, 411–427, 1992.

Schott, F., Pollehne, F., Quadfasel, D., Stramma, L., Wiesner, M., and Zeitschel, B.: ARABIAN SEA, Cruise No. 32, 23 March–19 September 1995, METEOR-Berichte, Universität Hamburg, 96-6, 163 pp, 1996.

Schubert, C. J., Villanueva, J., Calvert, S. E., Cowie, G. L., von Rad, U., Schulz, H., Berner, U., and Erlenkeuser, H.: Stable phytoplankton community structure in the Arabian Sea over the last 200 000 years, Nature, 394, 563–566, 1998.

Schultheiss, P. J. and Weaver, P. P. E.: Multi-sensor core logging for science and industry. In: Proceedings Oceans 92, Mastering the Oceans Through Technology, 2, 608–613, 1992.

Schulte, S., Mangelsdorf, K., and Rullkötter, J.: Organic matter preservation on the Pakistan continental margin as revealed by biomarker geochemistry, Org. Geochem., 31, 1005–1022, 2000.

Schulz, H., von Rad, U., and von Stackelberg, U.: Laminated sediments from the oxygen-minimum zone of the northeastern Arabian Sea, in: Paleoclimatology and Paleoceanography from Laminated Sediments, edited by: Kemp, A. E. S., Geol. Soc. Spec. Publ., 116, 185–207, 1996.

Schulz, H., von Rad, U., and Ittekkot, V.: Planktic foraminifera, particle flux and oceanic productivity off Pakistan, NE Arabian Sea: modern analogues and application to the paleorecord, in: The Tectonic and Climatic Evolution of the Arabian Sea Region, edited by: Clift, P. D., Kroon, D., Gaedicke, C., and Craig, J., Geol. Soc. Spec. Publ., 195, 499–516, 2002.

Sirocko F. and Sarnthein, M.: Wind-borne deposits in the northwestern Indian Ocean: record of Holocene sediment versus modern satellite data, edited by: Leinen, M. and Sarnthein, M., NATO ASI Series C, 282, 401–433, 1989.

Suthhof, A., Jennerjahn, T. C., Schäfer, P., and Ittekkot, V.: Nature of organic matter in surface sediments from the Pakistan continental margin and the deep Arabian Sea: amino acids, Deep-Sea Res. Pt. II, 47, 329–351, 2000.

Tiemann, J.: Korngrößen und mineralogische Zusammensetzung von Sinkstoffen und Oberflächensedimenten aus dem Arabischen Meer – Hinweise auf Quellen und Transport des Lithogenen Materials, Dissertation, Fachbereich Geowissenschaften, Universität Hamburg, Hamburg, März 2001, 120 pp + App., 2001.

Thiede, J., Suess, E., and Müller, P. J.: Late Quaternary Fluxes of Major Sediment Components to the Sea Floor at the Northwest African Continental Slope, in: Geology of the Northwest African Continental Margin, edited by: von Rad, U., Hinz, K., Sarnthein, M., and Seibold, E., Springer Verlag, 605–631, 1982.

van der Weijden, C. H., Reichart., G. J., and Visser, H. J.: Enhanced preservation of organic matter in sediments deposited within the oxygen-minimum zone in the northeastern Arabian Sea, Deep-Sea Res., 46, 807–830, 1999.

von Rad, U., Schulz, H., and SONNE 90 Scientific Party: Sampling the Oxygen Minimum Zone off Pakistan: Glacial/Interglacial variations of anoxia and productivity, Mar. Geol., 125, 7–19, 1995.

von Rad, U., Doose-Rolinski, H., and Scientific Shipboard Party SO 130, Makran II: The Makran accretionary wedge off Pakistan: tectonic evolution and fluid migration.- Cruise report, 3.April–3.Mai 1998, Bundesanstalt für Geowissenschaften und Rohstoffe, Hannover, Archiv No. 117368, 152 pp + Appendix, 1998.

von Rad, U., Schaaf, M., Michels, K. H., Schulz, H., Berger, W. H., and Sirocko, F.: A 5000-year record of climate change in varved sediments from the Oxygen Minimum Zone off Pakistan, Northeastern Arabian Sea, Quat. Res., 51, 39–53, 1999.

von Stackelberg, U.: Faziesverteilung in Sedimenten des indisch-pakistanischen Kontinentalrandes (Arabisches Meer), “Meteor”-Forsch.-Ergebnisse, Reihe C, 9, 1–73, 1972.

Weber, M. E., Niessen, F., Kuhn, G., and Wiedecke, M.: Calibration and application of marine sedimentary physical properties using a multi-sensor core logger, Mar. Geol., 136, 151–172, 1997.

Žarić, S., Schulz, M., and Mulitza, S.: Global prediction of planktic foraminiferal fluxes from hydrographic and productivity data, Biogeosciences, 3, 187–207, doi:10.5194/bg-3-187-2006, 2006.

Zobel, B.: Biostratigraphische Untersuchungen an Sedimenten des indisch-pakistanischen Kontinentalrandes (Arabisches Meer), “Meteor” Forsch. Ergebnisse, Reihe C, 12, 9–73, 1973.

Title Page
Abstract Introduction
Conclusions References
Tables Figures
|◀ ▶|
◀ ▶
Back Close
Full Screen / Esc
Printer-friendly Version
Interactive Discussion

Table 1. List of radiocarbon AMS-dates from latest Holocene laminated sediments of the oxygen minimum zone OMZ off Pakistan (see page 13).

Number	Sample	Corrected pMC	Conventional Age (yr)	Varve age (yr)*	Reservoir age (yr)
KIA201	M32-2MC1, 0–5 cm	100.42 +/−0.33	> 1950 AD	1970	–
KIA202	M32-2MC1, 18.5–22.5 cm	91.12 +/−0.31	747 + 27/−27 BP	1820	582
KIA773	M32-2MC5, 0–2.5 cm	105.05 +/−0.41	> 1950 AD	1984	–
KIA774	M32-2MC5, 15–18.5 cm	92.06 +/−0.32	664 + 28 /−28 BP	1903	572
KIA775	M32-2 MC5, 26–28 cm	91.59 +/−0.30	705 + 27/−27 BP	1867	577

assuming constant sedimentation rates (Table 2).

Table 2. List of fluxes of lithic matter, calcium carbonate (CaCO$_3$), and organic carbon (OC) in the water column sediment traps EPT1, EPT2, WPTs, and WPTd and reconstructed accumulation rates AR at the seafloor for 16 short cores at water depths of 196 m–1970 m.

(a) Particle Flux

Trap	Depth (m)	Sampling start	Sampling end	Sampling (d)	Total Flux (mg m^{-2} d^{-1})	Lith. Flux (mg m^{-2} d^{-1})	CaCO$_3$ Flux (mg m^{-2} d^{-1})	Opal Flux (mg m^{-2} d^{-1})	OC Flux (mg m^{-2} d^{-1})	Lith. Flux (%)	CaCO$_3$ Flux (%)	Opal Flux (%)	OC Flux (%)
EPT1-01	590	15/10/93	05/11/93	22	504	282	108	45	38	55.96	11.09	4.60	3.90
EPT1-02	590	06/11/93	27/11/93	22	680	464	138	43	19	68.28	10.28	3.17	1.44
EPT1-03	590	28/11/93	19/12/93	22	1086	769	164	73	45	70.77	7.66	3.43	2.09
EPT1-04	590	20/12/93	10/01/94	22	4848	3621	713	351	91	74.68	7.41	3.65	0.94
EPT1-05	590	11/01/94	01/02/94	22	4298	3234	639	297	71	75.25	7.48	3.48	0.83
EPT1-06	590	02/02/94	23/02/94	22	3501	2609	523	256	63	74.53	7.52	3.68	0.91
EPT2-01	590	05/05/95	29/05/95	24	1678	1081	404	111	45	64.45	12.16	3.35	1.37
EPT2-02	590	30/05/95	23/06/95	24	501	326	96	42	21	65.07	9.70	4.22	2.13
EPT2-03	590	24/06/95	18/07/95	24	688	484	109	51	24	70.43	8.02	3.78	1.77
EPT2-04	590	19/07/95	12/08/95	24	188	126	32	15	8	67.05	8.73	4.19	2.13
EPT2-05	590	13/08/95	06/09/95	24	1337	1012	148	107	39	75.67	5.60	4.07	1.47
EPT2-06	590	07/09/95	01/10/95	24	2444	1841	225	226	84	75.34	4.66	4.70	1.75
EPT2-07	590	02/10/95	26/10/95	24	160	106	25	12	9	66.11	7.99	3.99	2.99
EPT2-08	590	27/10/95	20/11/95	24	142	90	26	10	9	63.30	9.46	3.67	3.16
EPT2-09	590	21/11/95	15/12/95	24	136	88	24	9	8	65.15	9.05	3.36	3.02
EPT2-10	590	16/12/95	09/01/96	24	276	190	44	20	12	68.78	8.16	3.67	2.25
EPT2-11	590	10/01/96	03/02/96	24	4296	3270	598	269	89	76.11	7.02	3.15	1.04
EPT2-12	590	04/02/96	28/02/96	24	4077	3124	530	281	79	76.63	6.56	3.47	0.97
WPTS1-01	534	15/10/93	05/11/93	22	213	116	57	18	13	54.32	13.59	4.32	3.04
WPTS1-02	534	06/11/93	27/11/93	22	528	362	97	33	21	68.43	9.31	3.17	1.97
WPTS1-03	534	28/11/93	19/12/93	22	413	230	103	39	23	55.61	12.80	4.83	2.81
WPTS1-04	534	20/12/93	10/01/94	22	1424	994	224	127	44	69.79	7.95	4.53	1.56
WPTS1-05	534	11/01/94	01/02/94	22	5105	3870	738	334	90	75.82	7.28	3.30	0.89
WPTS1-06	534	02/02/94	23/02/94	22	1564	1094	258	143	38	69.95	8.33	4.61	1.24
WPTD1-01	1466	15/10/93	05/11/93	22	353	205	74	39	20	58.18	10.67	5.59	2.85
WPTD1-02	1466	06/11/93	27/11/93	22	485	332	84	37	18	68.48	8.76	3.92	1.84
WPTD1-03	1466	28/11/93	19/12/93	22	471	292	94	46	22	61.90	10.17	4.94	2.39
WPTD1-04	1466	20/12/93	10/01/94	22	199	119	45	21	8	59.53	11.45	5.44	2.04

(b) Sediment flux data

Cruise	Core	Latitude	Longitude	Water Depth (m)	Bulk-AR (mg m^{-2} d^{-1})	Lith.-AR (mg m^{-2} d^{-1})	CaCO3-AR (mg m^{-2} d^{-1})	Opal Flux (mg m^{-2} d^{-1})	OC-AR (mg m^{-2} d^{-1})	Lith. (%)	CaCO$_3$ (%)	Opal* (%)	OC (%)
METEOR 32/2	MC2	24° N 37.9′	66° E 06.4′	196	4187	2934	1178	167	75	70.08	28	4.00	1.79
METEOR 32/2	MC3	24° N 37.9′	66° E 04.6′	247	4369	3367	910	201	92	77.06	21	4.60	2.11
SONNE 90	44 KG	24° N 37.0′	66° E 01.5′	258	2200	1755	396	112	48	79.79	18	5.10	2.20
SONNE 90	42 KG	24° N 36.5′	65° E 59.0′	313	2193	1787	351	101	55	81.45	16	4.60	2.53
METEOR 32/2	MC5	24° N 38.4′	66° E 02.9′	386	2792	2272	454	137	66	81.36	16	4.90	2.37
METEOR 32/2	MC6	24° N 39.2′	66° E 01.0′	543	1227	1024	175	55	28	83.49	14	4.50	2.25
SONNE 90	39 KG	24° N 50.0′	65° E 55.0′	704	2891	2535	318	159	38	87.70	11	5.50	1.31
SONNE 90	53 KG	24° N 48.6′	65° E 55.0′	825	2735	2363	328	129	44	86.41	12	4.70	1.61
SONNE 90	58 KG	24° N 46.6′	65° E 49.2′	876	2764	2392	332	141	40	86.54	12	5.10	1.44
SONNE 90	76 KG	24° N 40.6′	65° E 41.2′	1168	956	831	115	45	9	86.97	12	4.70	0,99
METEOR 32/2	MC1	24° N 44.8′	65° E 46.6′	1266	2087	1805	250	94	31	86.50	12	4.50	1.50
SONNE 90	143 KG	24° N 45.0′	65° E 44.3′	1281	1217	1059	146	63	12	87.04	12	5.20	0.95
SONNE 90	72 KG	24° N 39.1′	65° E 45.4′	1403	1440	1240	187	73	13	86.13	13	5.10	0.88
SONNE 90	46 KG	24° N 33.2′	65° E 41.8′	1657	975	850	117	53	8	87.14	12	5.40	0.86
SONNE 90	144 KG	24° N 36.4′	65° E 35.1′	1943	1076	947	119	56	11	87.98	11	5.20	0.98
SONNE 90	79 KG	24° N 36.0′	65° E 35.1′	1970	1753	1550	193	96	11	88.39	11	5.50	0.60

(b) ff.

Core	Water Depth (m)	O2-BW (mg l^{-1})	PP** (mg C m^{-2} d^{-1})
MC2	196	0.08	711
MC3	247	0.07	711
44 KG	258	0.07	709
42 KG	313	0.08	708
MC5	386	0.06	714
MC6	543	0.05	716
39 KG	704	0.07	758
53 KG	825	0.07	753
58 KG	876	0.11	739
76 KG	1168	0.19	717
MC1	1266	0.37	731
143 KG	1281	0.38	730
72 KG	1403	1.36	714
46 KG	1657	1.60	697
144 KG	1943	1.97	706
79 KG	1970	1.99	706

* Opal sedimentary concentration data taken from Suthhof et al., 2000.** Primary productivity from Antoine et al., 1996.

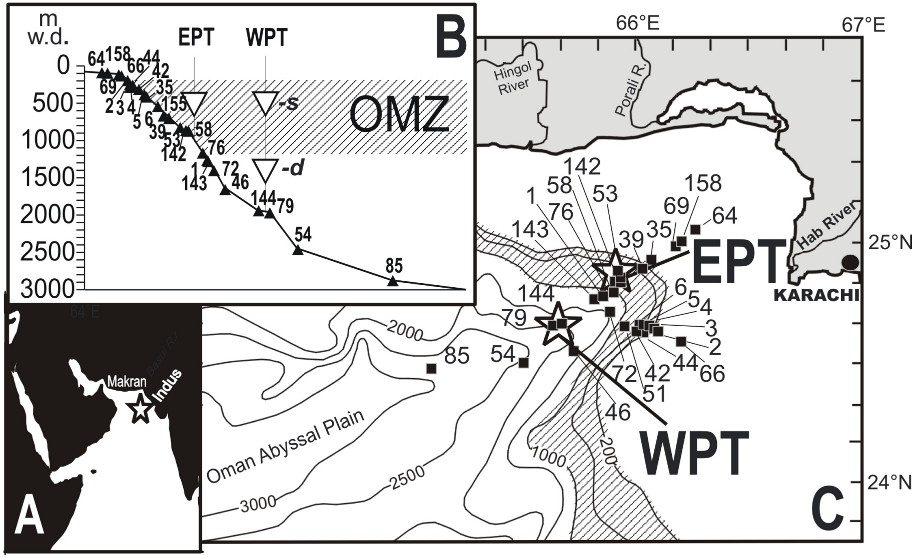

Fig. 1. Investigation area in the northwestern Indian Ocean off Pakistan. **(A)** Arabian Sea with Makran and Indus continental slopes; **(B)** Position of sediment traps and core top sediments (“Hab transect”) from two (pale)oceanographic cruises, SONNE 90 in 1993 (numbers 35ff.) and METEOR 32/2 in 1995 (numbers 1–6). Note that most sites are distributed below the narrow Makran shelf and some down the broader Indus margin. **(C)** Idealized transect of sediment stations between 92 m and 2881 m with sediment traps EPT and WPT. Distance between traps is ~20 km. Stippled area is the oxygen minimum zone, OMZ.

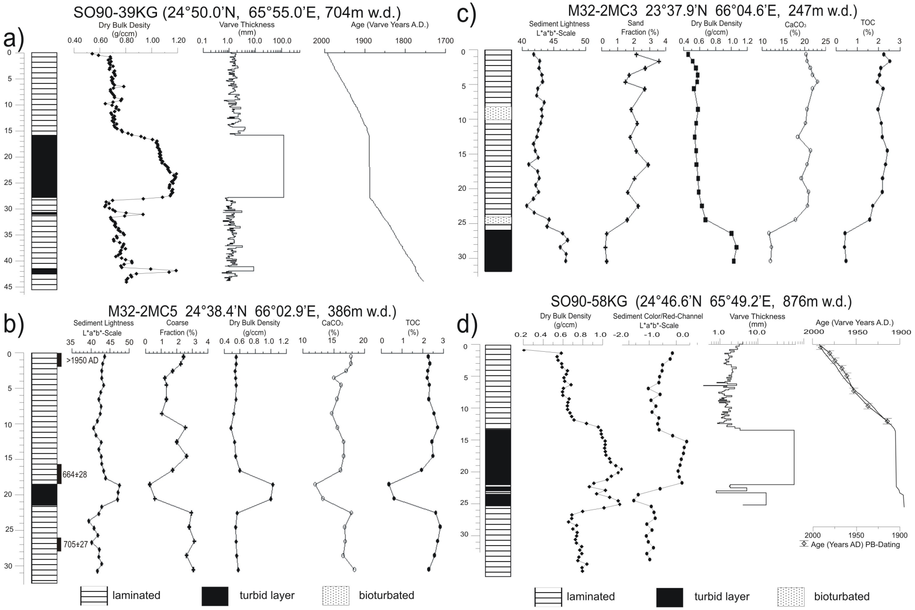

Fig. 2. Examples from four short sediment cores along the Pakistan margin for high-resolution analyses of sediment properties and dating. Various sediment properties display marked changes because of a 4 to 10 cm-thick turbid layer deposit. Profiles from the OMZ show distinct sediment laminations. According to models of their formation, varve counts, ^{14}C-, and ^{210}Pb dating provide and a coherent age of 1905–1888 AD for that layer.

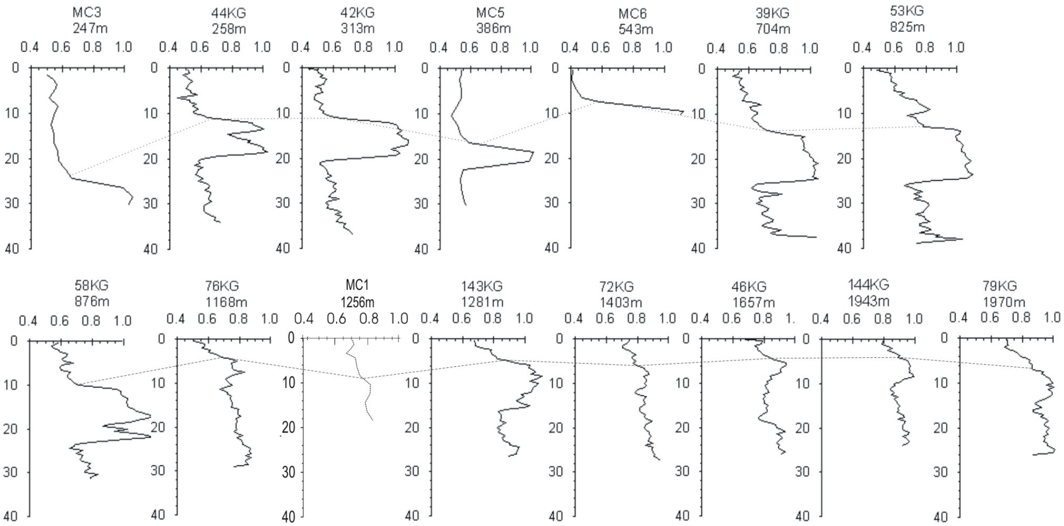

Fig. 3. Correlation of undisturbed short box (KG) and multicores (MC) cores by means of their sediment density profiles. A sudden increase in density (here expressed as dry bulk density) with depth (in cm) is evident for the laminated cores within the OMZ; density in lowest in the core top interval, and increase with depth by compaction below OMZ depths, this boundary is smoothed by bioturbation, but still present, fainting with water depth and distance from the margin.

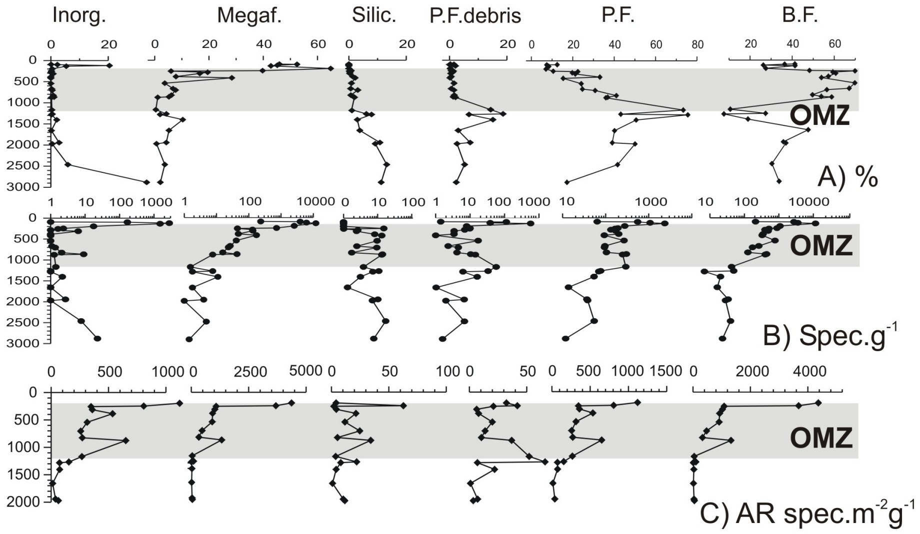

Fig. 4. Main components (in number of particles per gram dry sediment) of the coarse fraction (> 150 µm) down the Hab transect (see Fig. 1c). Inorg. = lithogenic and authigenic particles (quartz, concretions, pyrite, etc.); Megaf. = megafossils (mussels, snails, fish, etc.); Silic. = siliceous biogenic particles (radiolaria, diatoms, sponge spicules), P.F.debris = fragments of planktonic foraminifera; P.F. = planktonic foraminifera; B.F. = benthic foraminifera and fragments. The rows display **(A)** relative, **(B)** concentration, and **(C)** accumulation rates of the 6 categories. OMZ = oxygen minimum zone.

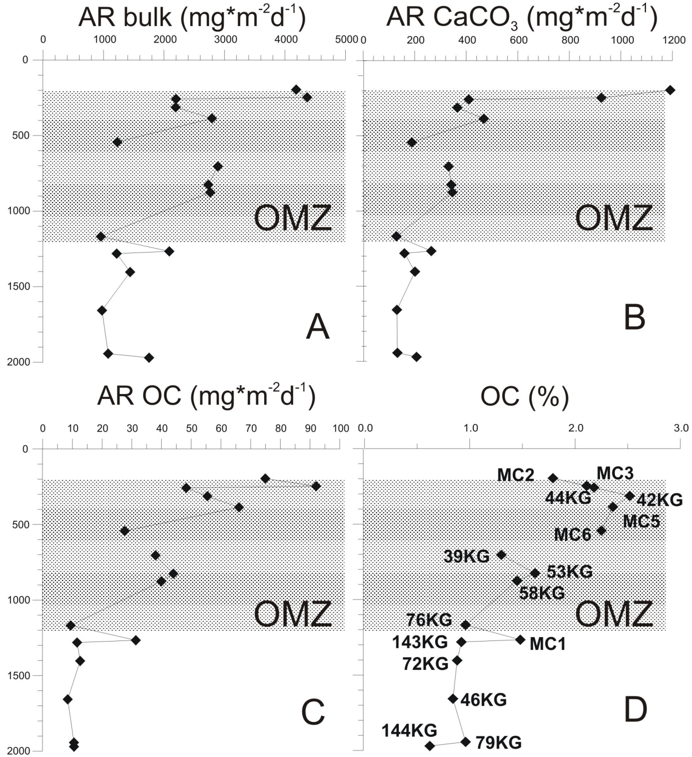

Fig. 5. Estimated accumulation rates (AR) of selected bulk parameters vs. water depth. Note that upper stations are on the Indus side, whereas the deeper cores are on the Makran. **(A)** AR bulk; **(B)** AR $CaCO_3$; **(C)** AR OC, **(D)** OC%. Stippled area is OMZ between ∼ 200–1200 m water depth.

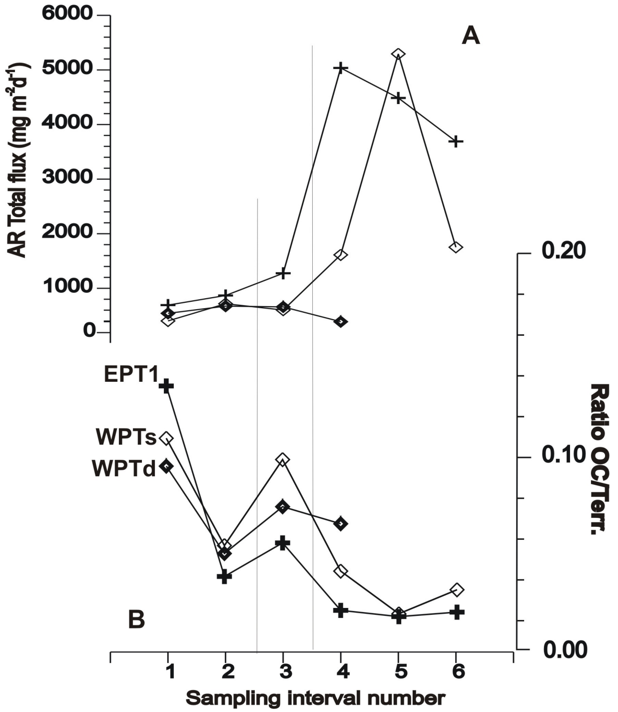

Fig. 6. Details of flux recording prior and during to the winter high flux events (HFE) from tree sediment traps (EPT, WPTs and WPTd) with synchronous collection periods (Andruleit et al, 2000). **(A)** differences in the timing of increase and peak flux in the shallow traps EPT and WPTs). **(B)** composition of settling flux (ratio of OC/lithic). All traps display similar compositions (Lithic = 86–94 %) prior to the HFE disturbance between collecting intervals 3 and 4 with an increase of lithic matter (> 95 %.). Lithic fraction is highest in EPT for the HFE with 98 % in sampling numbers 4, 5, 6.

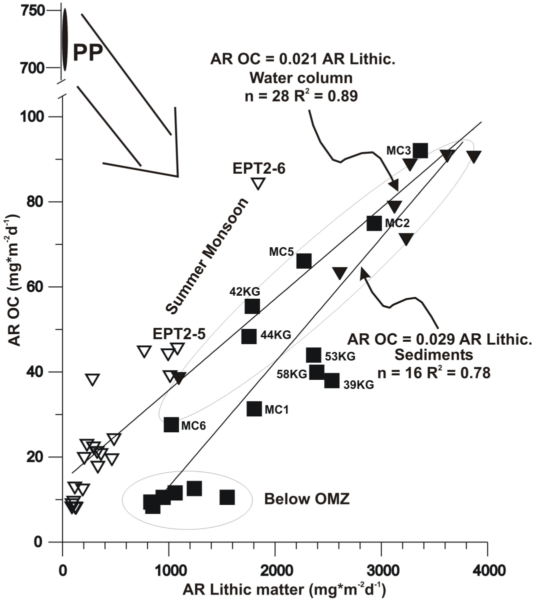

Fig. 7. Flux and composition of sedimentary and settling matter within and below the OMZ off Pakistan (Makran, Hab transect). Yearly average in primary production (PP) at all sites is 700–750 mg OC m^{-2} d^{-1} (Antoine et al., 1996) and dust input to the lithic fraction off Pakistan is low (~ 40 mg m^{-2} d^{-1}; Tiemann, 2001). Flux rates of settling and sediment matter is between ~ 10 and 100 mg OC m^{-2} d^{-1} with rather stable ratios to lithic matter (water column $R^2 = 0.89$ and sea floor $R^2 = 0.78$). With the onset of SW – monsoonal productivity in the area (sample EPT2-5 – EPT2-6), fraction of OC in summer and fall is enhanced (see Table 2). HFE-flux (gray triangles) and shelf sediments (black squares) plot together in their low OC/Lithic ratios, suggesting that the winter flux represents remobilized matter from the shelf. Sediment matter from deeper sites and from below the OMZ may reflect a relative loss of OC by degradation, compared to the flux samples.

Title Page
Abstract | Introduction
Conclusions | References
Tables | Figures
◀◀ | ▶▶
◀ | ▶
Back | Close
Full Screen / Esc
Printer-friendly Version
Interactive Discussion